Mouse dyskerin mutations affect accumulation of telomerase RNA and small nucleolar RNA, telomerase activity, and ribosomal RNA processing

Yuko Mochizuki*, Jun He*, Shashikant Kulkarni*, Monica Bessler*†, and Philip J. Mason*‡

*Department of Internal Medicine, Division of Hematology, Washington University School of Medicine, St Louis, MO 63110; and ‡Department of Haematology, Imperial College School of Medicine, Hammersmith Hospital, Du Cane Road, London W12 ONN, United Kingdom

Edited by Joan A. Steitz, Yale University, New Haven, CT, and approved June 8, 2004 (received for review April 9, 2004)

Dyskerin is a nucleolar protein present in small nucleolar ribonucleoprotein particles that modify specific uridine residues of rRNA by converting them to pseudouridine. Dyskerin is also a component of the telomerase complex. Point mutations in the human gene encoding dyskerin cause the skin and bone marrow failure syndrome dyskeratosis congenita (DC). To test the extent to which disruption of pseudouridylation or telomerase activity may contribute to the pathogenesis of DC, we introduced two dyskerin mutations into murine embryonic stem cells. The A353V mutation is the most frequent mutation in patients with X-linked DC, whereas the G402E mutation was identified in a single family. The A353V, but not the G402E, mutation led to severe destabilization of telomerase RNA, a reduction in telomerase activity, and a significant continuous loss of telomere length with increasing numbers of cell divisions during *in vitro* culture. Both mutations caused a defect in overall pseudouridylation and a small but detectable decrease in the rate of pre-rRNA processing. In addition, both mutant embryonic stem cell lines showed a decrease in the accumulation of a subset of H/ACA small nucleolar RNAs, correlating with a significant decrease in site-specific pseudouridylation efficiency. Interestingly, the H/ACA snoRNAs decreased in the G402E mutant cell line differed from those affected in A353V mutant cells. Hence, our findings show that point mutations in dyskerin may affect both the telomerase and pseudouridylation pathways and the extent to which these functions are altered can vary for different mutations.

The nucleolar protein dyskerin is one of four proteins associated with H/ACA small nucleolar RNA (snoRNAs) in small nucleolar ribonucleoprotein particles that catalyze the pseudouridylation of specific uridine residues during the maturation of rRNAs (1, 2). Dyskerin has similarities with yeast and bacterial pseudouridine synthases, suggesting that it is the active enzyme (3–7). The H/ACA snoRNAs act as guide RNAs that target the complex to specific residues via specific base pairing (8, 9). Telomerase (10, 11), which spends part of its time in the nucleolus (12, 13), is a ribonucleoprotein complex whose core components are the telomerase reverse transcriptase TERT and the telomerase RNA component *TERC*, which acts as a template for the synthesis of the TTAGGG telomere repeats at the ends of chromosomes. These simple repeats, along with a number of associated proteins, protect the ends of chromosomes from degradation and aberrant fusion events. *TERC* has a H/ACA like domain at its 3′ end (12) and is associated with the same four proteins as H/ACA snoRNAs, including dyskerin (14–16). Because no pseudouridylation target associated with telomerase action has been identified, it is assumed that dyskerin has a structural role in the telomerase complex.

X-linked dyskeratosis congenita (DC), caused by point mutations in the *DKC1* gene that encodes dyskerin (17), is a rare, usually fatal, inherited skin and bone marrow failure syndrome in which patients develop mucocutaneous lesions, aplastic anemia, and an increased susceptibility to cancer (18, 19). Tissues with a rapid cell turnover appear to be the main target of the DC pathobiology (20, 21). It is not clear whether the function of dyskerin as a pseudouridine (Ψ) synthase, its role in the telomerase complex, or both, is primarily responsible for the pathogenesis of DC. Although an autosomal form of DC is caused directly by mutations in *TERC* (22), suggesting that the disease is caused by defective telomerase activity, studies from animal models suggest that defective rRNA processing may cause some of the features of DC (23, 24). In this paper, we approach this controversy by inducing DC-causing point mutations in the highly conserved *Dkc1* gene of embryonic stem (ES) cells normally expressing high levels of dyskerin and telomerase activity. We show that these two dyskerin mutations may affect both telomerase and pseudouridylation, and that the extent to which these two processes are altered varies for the two mutations.

Materials and Methods

Preparation of Targeting Construct, Generation of A353V and G402E ES Cells, and Cell Culture. Targeting constructs were made by oligonucleotide-directed mutagenesis using the Transformer (Clontech) system and standard subcloning methods as described (25). ES cells (RW-4, Siteman Cancer Center at Washington University School of Medicine) were transfected with A353V or G402E targeting vector and selected with Geneticin (Sigma). A353V and G402E ES clones were cultured on mitomycin C-treated STO cell (ATCC CRL-2225) feeder layers in ES medium (DMEM, 17% FCS) supplemented with L-glutamine, nonessential amino acids, Hepes, leukemia inhibitory factor, and 2-mercaptoethanol.

RNA Isolation and Northern Blot Analysis. Total RNA was isolated from ES cells by using TRIzol (Invitrogen). For analysis of snoRNAs, 20 μg of total RNA was electrophoresed through 6% polyacrylamide/7 M urea gels and transferred onto Zeta-probe membranes (Bio-Rad) by using Transblot SD semidry blotting apparatus (Bio-Rad). The sequence of the oligonucleotides used to probe these blots is supplied in Table 1, which is published as supporting information on the PNAS web site.

Telomeric Repeat Amplification Protocol (TRAP) Assay. Telomerase activity was measured by using the TRAPeze telomerase detection kit (Intergen, Purchase, NY) according to the manufacturer's recommendations. Cell lysates were prepared by using the 3-[(3-cholamidopropyl)dimethylammonio]-1-propanesulfonate (CHAPS) lysis buffer provided in the kit and stored at −80°C. Protein concentration was measured in each extract by using the Bio-Rad Protein assay (Bio-Rad).

This paper was submitted directly (Track II) to the PNAS office.

Abbreviations: DC, dyskeratosis congenita; snoRNA, small nucleolar RNA; ES, embryonic stem; Ψ, pseudouridine; TRAP, telomeric repeat amplification protocol; IRES, internal ribosome entry site.

†To whom correspondence should be addressed. E-mail: mbessler@im.wustl.edu.

Analysis of Telomere Lengths (26). Cells were isolated and embedded in agarose plugs following instructions from the manufacturer (CHEF agarose plug kit; Bio-Rad). DNA embedded in the agarose plug was digested with *Mbo*I and electrophoresed through a 1% agarose gel for 23 h at 6 V/cm at a constant pulse time of 5 s using the CHEF DR-III pulse-field system. The gel was analyzed by in-gel hybridization with [^{32}P] 5′ end-labeled oligonucleotide $(CCCTAAA)_4$ probe.

Western Blot Analysis. Primary antibody incubations were carried out by using the antibody to TOPOIIβ (H-286; dilution 1:200; Santa Cruz Biotechnology) and polyclonal antiserum to dyskerin raised against the peptides DCSNPLKREIGDYIR (amino acids 74–88) and GLLDKHGKPTDNTPAC (amino acids 382–396+C; dilution 1:1,000) and supplied by Eurogentec (Brussels). Western blots were developed by using chemiluminescence (SuperSignal from Pierce).

Metabolic Labeling and Analysis of rRNA Processing. ES cells were plated in 35-mm-diameter plates at 2.0×10^6 cells per plate. The cells were incubated in medium with [^{3}H]uridine (ICN Biomedicals; 5 μCi/ml; 1 Ci = 37 GBq) for 30 min and then incubated in nonradioactive medium for 2 h.

For [*methyl*-^{3}H]methionine pulse–chase analysis, the cells were preincubated in methionine-free medium for 45 min, before being pulse-labeled with 50 μCi/ml [*methyl*-^{3}H]methionine (New England Nuclear), for 30 min and chased with cold methionine (30 μg/ml). Samples were taken every 15 min.

Total RNA (from 1.0×10^6 cells) was separated on a 1% agarose formaldehyde gel and transferred to a nylon membrane. The membranes were sprayed with EN^{3}HANCE Spray (New England Nuclear), dried, and exposed to x-ray films at −80°C.

Analysis of Pseudouridylation in 28S and 18S rRNA. ES cells were pretreated in phosphate-free medium for 1 h and labeled for 3 h with [^{32}P]orthophosphate (100 μCi/ml). Total RNA was electrophoresed through a 1% agarose formaldehyde gel. The 28S and 18S rRNA were purified by electroelution, phenol-chloroform extracted, ethanol precipitated, and digested with RNase T2 (Sigma) in 50 mM ammonium acetate, pH 4.5/0.05% SDS/1 mM EDTA at 37°C. Digested RNA (20,000 cpm each) was analyzed by two-dimensional cellulose TLC (EM Science, Gibbstown, NJ) by using isobutyric acid/NH_4OH/H_2O (577:38:385, by volume) in the first dimension and 2-propanol/HCl/H_2O (70:15:15, by volume) in the second dimension. Spots of uridine or Ψ were analyzed by Cerenkov counting, and Ψp/uridine ratios were determined.

***In Vitro* Assay of Pseudouridylation.** *In vitro* assays of pseudouridylation were performed as described (27). Site-specifically labeled rRNA substrates used in this study are shown in Fig. 5.

Labeling of the target uridine and oligodeoxynucleotide-mediated ligation were performed according to the two-way RNA ligation protocol (28). The position in the U19 substrate was deduced from that in human U19. RNA oligomers were synthesized and purified with RNase-free HPLC (Integrated DNA Technologies, Coralville, IA). The ligation products were purified by 12% urea PAGE. Preparation of nuclear extracts and the pseudouridylation assay were performed as described (27).

Results

Production of Mouse ES Cell Lines with *Dkc1* Point Mutations. We used gene trapping vectors containing an internal ribosome entry site (IRES)-NEO cassette in the *Dkc1* 3′ UTR to insert point mutations causing amino acid substitutions A353V and G402E into the mouse *Dkc1* locus (Fig. 1). ES cell clones that had recombined at the 3′ end but did not contain the *Dkc1*

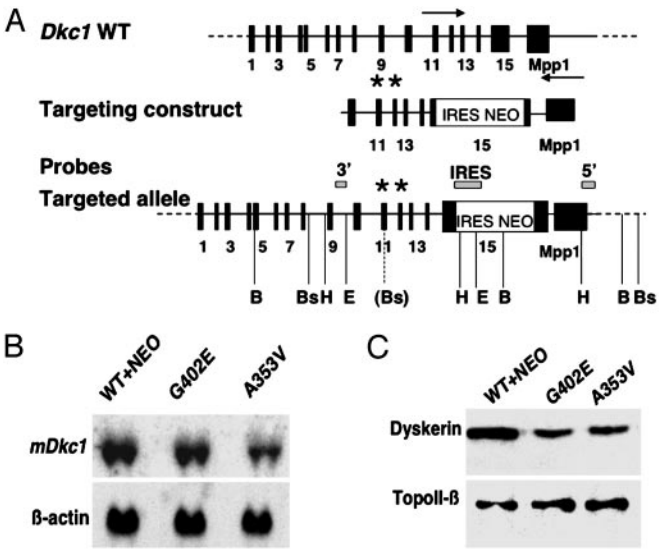

Fig. 1. Targeting the *Dkc1* locus in ES cells. (*A*) The targeting construct was a 6.5-kb *Eco*RI/*Hin*dIII fragment in which an IRES-Neo element had been cloned into a unique *Stu*I site in the 3′ untranslated region. The positions of the probes are shown. The asterisk represents the position of the mutations A353V and G402E in exons 11 and 12, respectively. The positions of restriction enzyme sites used in confirmatory Southern blots (not shown) are indicated; B, *Bam*HI; Bs, *Bsp*HI; H, *Hin*dIII; E, *Eco*RI. The Bs site in brackets is the site created with the A353V mutation. The probes were 5′, a single-copy 600-bp fragment from *Dkc1* intron 9; IRES, a 200-bp *Hin*dIII/*Kpn*I fragment from the IRES element; and 3′, a 500-bp *Bst*X1/*Hin*dIII fragment from Mpp1 cDNA. (*B*) Northern hybridization. RNA was extracted from ES cells containing the wild-type *Dkc1* gene with an IRES-NEO cassette in the 3′ untranslated region (WT+NEO) or ES cell clones targeted to contain point mutations as well as the IRES-NEO cassette (G402E and A353V). Twenty-five micrograms of total RNA was loaded in each lane and hybridized sequentially with probes for *Dkc1* and *β-actin*. (*C*) Western blotting of nuclear extracts from ES cells. Ten micrograms of protein was loaded in each lane. Expression of dyskerin was detected with anti-dyskerin antiserum. TopoII-β was detected with a specific antibody as a loading control.

point mutations (designated WT+NEO) were used to control for any effect of the IRES-NEO element in the 3′ UTR and for the presence of neomycin in the culture medium. We previously showed in mouse lines that the presence of the IRES-NEO element in the 3′ UTR of the *Dkc1* gene was not deleterious to the cells, although the biochemical analyses reported here were not carried out (25). All ES cell clones had a normal XY karyotype (data not shown). In culturing ES cells containing the mutations A353V or G402E for 400 population doublings, we did not observe any obvious difference in the growth rate of the mutant cells or any morphological changes in the cells compared to wild-type ES cells. Any differences that we observed between cell lines and reported below were found in at least two separate experiments and in at least two independent cell lines of each genotype. Northern blot analysis of RNA isolated from the mutant and control ES cells revealed a decrease in the abundance of dyskerin mRNA in the A353V cell lines compared to the WT+NEO control cells (Fig. 1*B*). Western blotting showed that both mutant cell lines consistently showed a reduced level of dyskerin with about half the level of the wild-type protein (Fig. 1*C*).

The A353V Mutation Causes a Decrease in *Terc* RNA Levels and in Telomerase Activity, Leading to Telomere Shortening. It is not known whether the decreased levels of *TERC* RNA, low levels of telomerase activity (14), and short telomeres (29) in cells from X-linked DC patients are a direct effect of the dyskerin muta-

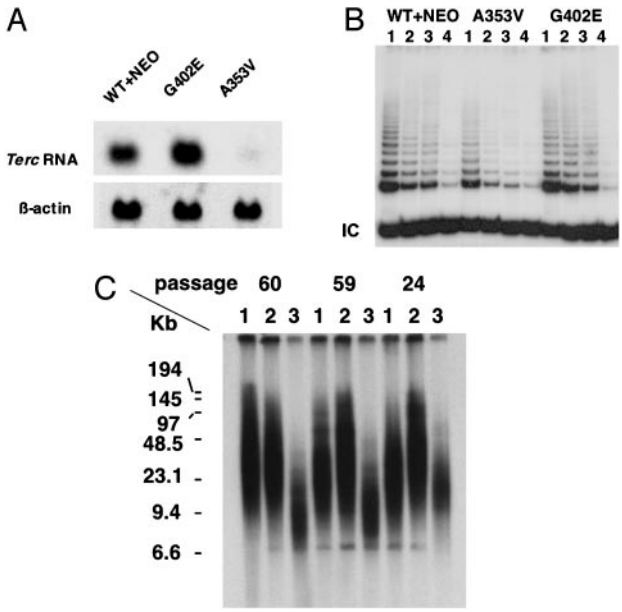

Fig. 2. The effect of point mutations in *Dkc1* on *Terc* RNA levels, telomerase activity, and telomere lengths. (*A*) Northern hybridization. RNA was extracted from ES cells containing the wild-type *Dkc1* gene (WT+NEO) or ES cell clones targeted to contain point mutations (G402E and A353V). Twenty-five micrograms of total RNA was loaded in each lane and hybridized sequentially with probes for *Terc* and *β-actin*. (*B*) Telomerase activity in ES cells. Extracts in 3-[(3-cholamidopropyl)dimethylammonio]-1-propanesulfonate (CHAPS) lysis buffer were prepared from *Dkc1* mutant and control ES cell clones. The TRAP assay for telomerase activity was performed on 2.0×10^{-2} (lane 1), 1.0×10^{-2} (lane 2), and 0.5×10^{-2} (lane 3) μg of protein. A total of 2.0×10^{-2} μg of protein from heat-treated samples was used as negative control (lane 4). IC, internal positive control for PCR. (*C*) Telomere lengths in ES cells. *Dkc1* mutant and control ES cell clones were passaged 60, 59, and 24 times. Telomeric terminal restriction fragments were analyzed by in-gel hybridization with a ^{32}P-end-labeled oligonucleotide (CCCTAA) probe. Lanes: 1, WT+NEO; 2, G402E; 3, A353V. The sizes of molecular mass markers are shown on the left.

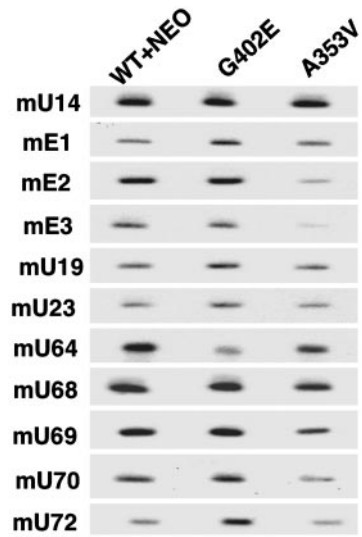

Fig. 3. The effect of *Dkc1* mutations on H/ACA snoRNAs. Twenty micrograms of total RNA was loaded in each lane of a Northern blot, and the membrane was hybridized sequentially with end-labeled oligonucleotide probes specific for the murine H/ACA snoRNA species indicated. The C/D box snoRNA U14 was used as a loading control.

tions or are a downstream consequence of the bone marrow failure in these patients. We analyzed levels of *Terc* RNA by Northern blotting in the ES cells carrying mutant *Dkc1* genes (Fig. 2*A*). We observed a dramatic decrease in *Terc* RNA levels in ES cells carrying the A353V mutation in *Dkc1*, whereas ES cells with the G402E mutation had apparently wild-type levels of *Terc* RNA. The decrease in *Terc* RNA levels in the A353V mutant was much greater than the decrease in dyskerin mRNA or protein levels seen in the mutant cell lines, and is therefore likely to be a specific effect of the amino acid substitution. This conclusion is strengthened by the fact that the G402E mutant cell lines show no reduction in *Terc* RNA levels, although they also show a decrease in the steady state level of dyskerin.

Next, we tested the effect of the dyskerin mutations on telomerase activity. We measured telomerase activity in cell lysates by using the semiquantitative TRAP assay. The results (Fig. 2*B*) show that telomerase activity in ES cells with A353V mutant dyskerin was considerably reduced (34% of WT+NEO), whereas the G402E mutation did not cause a significant reduction in activity. It was important to know whether the reduction in telomerase activity would lead to telomere shortening in ES cells. ES cells were subcultured to a dilution of 1:20 when confluent, approximately every 3 days. DNA was extracted after 24, 59, and 60 passages, and telomere length was measured by Southern blotting and in-gel hybridization. As shown in Fig. 2*C*, telomere lengths in the A353V ES cells were already shorter than in the control cells at 24 passages and were very short at 59 and 60 passages. The G402E cells and the WT+NEO cells, on the other hand, maintain their telomere length throughout the 60 passages. We conclude that the A353V mutation in dyskerin leads directly to defects in telomere maintenance by destabilizing *Terc* RNA.

Accumulation of H/ACA snoRNAs Is Altered in Cells with G402E or A353V Mutations in Dyskerin. Because stability of *Terc* RNA is mediated through its H/ACA domain, we considered that H/ACA snoRNAs may also be unstable in cells containing mutant dyskerin. We therefore examined the accumulation of H/ACA snoRNA in mutant ES cells by using Northern hybridization. We tested a series of mouse H/ACA snoRNAs that had characterized human homologues (30). Oligonucleotides complementary to the snoRNA sequences were used to probe Northern blots of total RNA from WT+NEO control cells and the two mutant ES cell lines. The results (Fig. 3) show some variability in the levels of snoRNAs; however, in the A353V cell line H/ACA snoRNAs mE2, mE3, mU68, mU69, and mU70 were consistently significantly decreased (in four separate experiments). The results from the G402E cell line were more complex, with mU64 decreased and mE1 and mU72 apparently increased in amount.

Total Ψ Is Decreased in 18S and 28S rRNA in *Dkc1* Mutant ES Cells. In yeast and *Drosophila*, mutations in dyskerin orthologs lead to a decrease in total Ψ content in rRNA (6, 23). The same has been found in mice with a hypomorphic mutation close to the *Dkc1* gene (24). Therefore, we asked whether the mutations in the *Dkc1* gene in mouse ES cells led to a decrease in the total amount of Ψ. ^{32}P-labeled 18S and 28S rRNA was obtained from mutant and control ES cell lines by labeling with [^{32}P]orthophosphate, RNA extraction, and gel purification. The RNAs were digested with RNase T2 before analysis of their nucleotide composition by two-dimensional TLC. Spots representing uridine and Ψ were carefully located and excised, and the radioactivity was counted. The results (Fig. 4) show that there is a significant decrease in the ratio of Ψ to uridine in both mutant cell lines. Thus, compared with a Ψ/uridine ratio of 100% in the WT+NEO cells, the values for 18S RNA were 82.8% (G402E) and 73.0% (A353V), whereas for 28S RNA, they were 70.9% (G402E) and

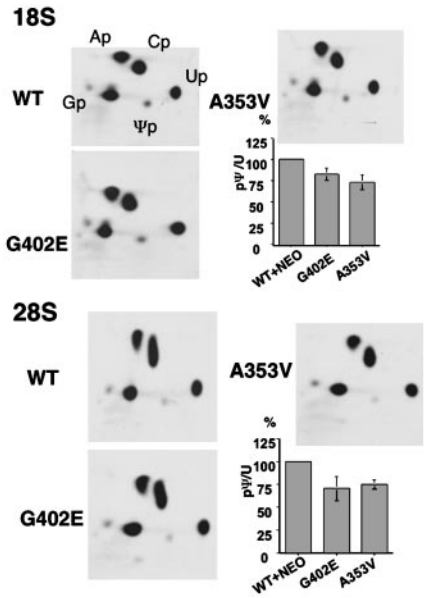

Fig. 4. Pseudouridylation in 18S or 28S rRNA from G402E and A353V ES cells. 18S and 28S rRNA of *Dkc1* mutant and control ES cells was labeled with ^{32}P-labeled orthophosphate, extracted, and gel-purified. After digestion with RNase T2, each sample was separated by two-dimensional TLC. The positions of the labeled ribonucleotides are indicated. From each TLC plate, spots of uridine (Up) and pseudouridine (Ψp) were excised and quantitated by Cerenkov counting. The ratio between incorporation into uridine and Ψp was calculated and is shown on the histogram where the WT+NEO, G402E, and A353V samples are compared with the WT+NEO sample (100%).

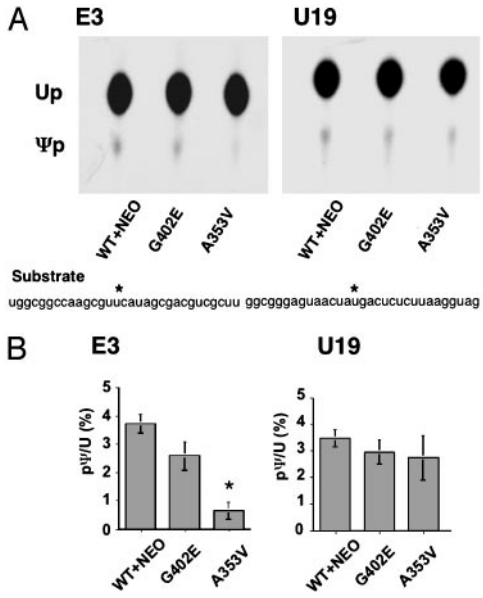

Fig. 5. Site-specific pseudouridylation of rRNA. (*A*) Nuclear extracts from targeted and control ES cell clones were incubated with labeled pseudouridylation templates. The sequence of ^{32}P-labeled oligo RNA substrates is shown. The asterisk indicates the positions of uridines that undergo pseudouridylation. Reactions were digested by RNase T2 and then separated by TLC. (*B*) The spots of uridine (Up) and Ψp were detected by autoradiography.

74.9% (A353V). The difference between WT+NEO and mutant cell lines was significant (*t* test, $P < 0.05$) and there was a significant difference between the two mutants for 18S (four independent clones tested) but not for 28S ($n = 5$).

Ψ Synthase Activity of A353V Dyskerin Mutants Was Reduced in an *in Vitro* Assay Using the H/ACA snoRNA E3 Target Uridine as Substrate. To test whether site-specific pseudouridylation is defective in A353V ES cells, we tested lysates from the mutant and control cell lines for their ability to carry out the pseudouridylation reaction *in vitro* (27). We chose to test a uridine residue, U4071 in 28S RNA, targeted by snoRNA mE3, which showed clearly decreased accumulation in the A353V cell line. As a control, we used a target uridine, U3419 in 28S RNA, of snoRNA U19, which was not altered in concentration in either of the mutant cell lines (see Fig. 3). We synthesized RNA templates with the appropriate uridine targets (8, 31), labeled with ^{32}P, and treated them with nuclear lysates from mutant and control ES cells (three independent clones of each type were used in these experiments). The amount of newly formed Ψ was then visualized after separation from uridine by one-dimensional TLC. The results (Fig. 5) show that there is a clear decrease in the amount of Ψ formed by the lysate from A353V cells. In the case of U19, no significant differences were detected. We conclude that in A353V mutant ES cells the efficiency of pseudouridylation of uridine 4071 is decreased.

Pre-rRNA Processing Intermediates Accumulate in *Dkc1* Mutant ES Cells. In yeast and *Drosophila*, mutations in dyskerin orthologs cause defects in the pre-rRNA processing pathway leading to a reduced rate of production of mature rRNAs and accumulation of unspliced precursor molecules (5, 6, 23). Similar observations have been made in mice with a hypomorphic mutation close to the *Dkc1* gene (24). We wished to know whether the dyskerin mutant ES cells had any pre-rRNA processing defects. Inefficient rRNA processing may arise as a consequence of decreased pseudouridylation of precursor rRNAs or decreased levels of those snoRNAs that mediate cleavage events during processing. Labeling RNA with [^{3}H]uridine did not show any differences in the accumulation of mature 18S and 28S rRNA (Fig. 6*A*), but indicated a slightly higher level of accumulated precursor molecules in the mutants compared with the WT+NEO cells. To further investigate this, we performed pulse–chase experiments using [^{3}H-*methyl*]methionine as the label, because of the rapid turnover of cellular methionine pools. The result (Fig. 6*B*) shows that, in cells containing either *Dkc1* A353V or *Dkc1* G402E, accumulation of labeled 45/47S and 32S precursors is seen to be markedly higher than in WT+NEO control cells.

Discussion

Although dyskerin and its role in pseudouridylation is evolutionarily highly conserved, it is only associated with telomerase in vertebrates (12, 16), where it may play a structural role, because no pseudouridylation targets are evident in the telomerase pathway. Thus, mutations in dyskerin could alter the stability of the RNA or the RNP complex as a whole or could specifically affect pseudouridylation. DC primarily affects tissues with rapidly dividing cells, so the pathology of DC is thought to be due to the effect of mutant dyskerin on stem cell and progenitor cell renewal (19, 21). Murine ES cells are untransformed, diploid, mammalian stem cells that express high levels of dyskerin and telomerase activity. In addition, specific mutations may be readily introduced into the ES cell genome. Hence, murine ES cells carrying pathogenic DC mutations are an ideal surrogate to evaluate the effect of the mutation on the dual function of dyskerin in rapidly dividing stem cells. The dyskerin mutation A353V analyzed here is the most frequent mutation in X-linked DC patients (19), whereas the G402E mutation has been described in a single family with typical DC (17).

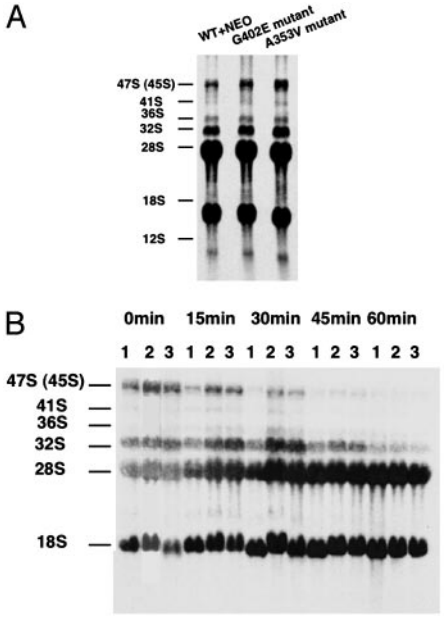

Fig. 6. The effect of *Dkc1* mutations on rRNA processing. (*A*) rRNA was labeled with 5 μCi/ml ^{3}H-labeled uridine for 30 min, then incubated in nonradioactive media for 2 h. In both experiments, RNA was extracted, loaded according to cell number (1.0×10^6 cells), and separated through 1% agarose formaldehyde gel. (*B*) Pulse–chase labeling experiment. Cells were labeled with 50 μCi/ml ^{3}H-labeled methyl methionine for 30 min and chased in cold methionine for 15, 30, 45, and 60 min. Lanes: 1, WT+NEO; 2, G402E; 3, A353V. The sizes of the processing intermediates and the mature RNA species are indicated at the left.

We find that the A353V mutation affects *Terc* RNA stability, the stability of specific snoRNAs, and the function of both *Terc* RNA and specific H/ACA snoRNAs. The A353V mutation is within the Ψ synthase and archeosine transglycosylase (PUA) RNA binding domain of the protein and is within a highly conserved motif. The *Drosophila* homolog 60B also has an alanine residue at this position (23). Interestingly, the yeasts *Saccharomyces cerevisiae* and *Schizosaccharomyces pombe,* in which dyskerin does not associate with the telomerase complex, both have a valine at the corresponding position (32). Thus, the A353V mutation is likely to affect RNA stability of *TERC* RNA and of a specific subset of snoRNAs, and exert its effects on telomerase and pseudouridylation/rRNA processing via these unstable RNAs.

If the A353V mutation affects the stability of the RNAs to which it binds, why does it affect them differently? Either the RNA species interact in a sequence-specific manner with the dyskerin protein, so that altering dyskerin residues may affect a subset of RNAs, or all RNAs are destabilized by the mutation in dyskerin, but a more dramatic effect is seen with RNAs with a longer half life. In support of this latter notion, the RNA most severely affected by the A353V mutation is the *Terc* RNA itself and human *TERC* RNA has been shown to be the longest lived RNA on record, with a half-life varying between 5 days and 4 weeks in different human cell lines (33). Little is known about the half-life of other snoRNAs.

Although the G402E mutation lies outside the PUA domain, it alters a conserved residue in a less conserved part of the protein; no function has been assigned to this part of dyskerin. Our results suggest that it may affect the accumulation of some specific snoRNAs that are different from the snoRNAs affected by the A353V mutation. However, the G402E mutation seems to affect total Ψ levels and decrease rRNA processing in the same way as A353V. It is possible that these overall effects are mediated by altered binding of as yet unknown snoRNAs common to both mutant cell lines. Although the majority of H/ACA snoRNAs so far described mediate pseudouridylation, some catalyze cleavage events in rRNA processing directly (34, 35).

The A353V mutant cells, but not the control or the G402E cells, consistently showed a decrease in the amount of dyskerin mRNA, suggesting a specific effect of the A353V mutation on mRNA stability. Both mutations lead to decreased amounts of dyskerin protein, suggesting that the mutant proteins are somewhat unstable. The lower amount of dyskerin, which was found in both mutant cell lines, cannot explain the effects on *Terc* RNA of the A353V mutation, because they were not seen with the G402E mutation. However, decreased protein levels could be responsible for the lowered rate of rRNA processing and the decreased level of total pseudouridylation.

An alternative, probably more trivial explanation for the differences we see between A353V and G402E mutant cells may be that, although the A353V mutation has a similar effect on the mouse protein as the same mutation has on the human protein, this may not apply to the G402E mutation. It is possible that in the different molecular environment of the murine protein the mutation is buffered from severely altering the spatial arrangement of the important functional residues.

In the A353V mutant cells, we observe severe telomere shortening without an observable effect on growth rate after 60 passages (equivalent to 270 population doublings). This is consistent with the observations of Niida *et al.* (36), who found ES cells with no telomerase activity (*Terc*−/−) grew normally for 300 divisions. It would be interesting to directly compare telomere dynamics in A353V versus *Terc*−/− ES cells for a large number of cell divisions to determine whether the residual activity in A353V cells may lead to the maintenance of short telomeres as has been found in *Tert*+/− mice (37).

An important issue concerns the role of defective dyskerin in the pathogenesis of dyskeratosis congenita. The results presented here show that both mutations lead to a decreased overall pseudouridylation and retard the rate of rRNA processing. Moreover, significant defects in specific snoRNA abundance are found in both mutant cells, and we demonstrate a corresponding deficiency in pseudouridylation at a specific site. Only the A353V mutation greatly reduces telomerase activity and leads to short telomeres, whereas the G402E mutation has no such effect. In contrast, Mitchell *et al.* (14), studying primary cells from two DC patients, found decreased *TERC* RNA and telomerase levels in both, but failed to find any defects in the accumulation of other H/ACA snoRNAs, pseudouridylation, or rRNA processing. How can these results be reconciled with ours? Apart from the mouse/human difference, the cell lines used by Mitchell *et al.* both carry mutations in the 5′ region of dyskerin with no assigned function. The effect of mutations in this region might differ from the effect of the mutations studied here. Alternatively, they may represent particularly mild DC variants, because cell lines from DC patients are notoriously difficult to grow. In these mild variants, in contrast to the more severe A353V variant, pseudouridylation defects or defects in rRNA processing may be very mild and not detected by the methods used. Indeed, we were only able to detect differences in rRNA processing by using a sensitive pulse–chase assay.

Currently, it is difficult to predict how the biochemical defect caused by the individual mutation will correlate with the clinical phenotype. The mutation A353V analyzed here is the most frequent mutation in X-linked DC patients (19). The disease is heterogeneous in its expression, even within patients carrying the same mutation (19). Patients with the A353V mutation vary in phenotype from typical DC, with signs of the disease appearing in the early childhood and severe bone marrow failure developing in the late teens, to very severe with

bone marrow failure, immune deficiency, and cerebellar hyperplasia (Hoyeraal–Hreidarsson syndrome, refs. 38 and 39) being evident within the first year. This finding suggests that additional genetic or environmental factors may play a role in disease expression. Only one family with the G402E mutation has been described and the patient in this case presented with typical DC (17). It is possible that the milder biochemical effects of the G402E mutation are reflected in the milder DC phenotype. The biochemical study of more pathogenic dyskerin mutations will be necessary to determine whether the biochemical defect defined in ES cells will correlate with the clinical phenotype seen in humans and to further define the key events in the molecular pathogenesis of bone marrow failure in DC.

We thank Sean Eddy for help in the analysis of snoRNA, Karen S. Hathcock for protocol for mouse telomere length analysis, and Inderjeet Dokal and Tom Vulliamy for helpful discussions. This work was supported by the Mallinkrodt Foundation, National Institutes of Health Grant RO1-CA-89091, American Cancer Society Grant IRG-58-010-41, and a Project grant and a subsequent Program grant from the Wellcome Trust. We thank the Alvin J. Siteman Cancer Center at Washington University School of Medicine (St. Louis) for the use of the Embryonic Stem Cell Core providing ES cell services (National Cancer Institute Cancer Center Support Grant P30 CA91842).

1. Filipowicz, W. & Pogacic, V. (2002) *Curr. Opin. Cell Biol.* **14,** 319–327.
2. Kiss, T. (2002) *Cell* **109,** 145–148.
3. Jiang, W., Middleton, K., Yoon, H. J., Fouquet, C. & Carbon, J. (1993) *Mol. Cell. Biol.* **13,** 4884–4893.
4. Meier, U. T. & Blobel, G. (1994) *J. Cell Biol.* **127,** 1505–1514.
5. Cadwell, C., Yoon, H. J., Zebarjadian, Y. & Carbon, J. (1997) *Mol. Cell. Biol.* **17,** 6175–6183.
6. Lafontaine, D. L., Bousquet-Antonelli, C., Henry, Y., Caizergues-Ferrer, M. & Tollervey, D. (1998) *Genes Dev.* **12,** 527–537.
7. Zebarjadian, Y., King, T., Fournier, M. J., Clarke, L. & Carbon, J. (1999) *Mol. Cell. Biol.* **19,** 7461–7472.
8. Ganot, P., Bortolin, M. L. & Kiss, T. (1997) *Cell* **89,** 799–809.
9. Kiss, T. (2001) *EMBO J.* **20,** 3617–3622.
10. Greider, C. W. & Blackburn, E. H. (1985) *Cell* **43,** 405–413.
11. Collins, K. & Mitchell, J. R. (2002) *Oncogene* **21,** 564–579.
12. Mitchell, J. R., Cheng, J. & Collins, K. (1999) *Mol. Cell. Biol.* **19,** 567–576.
13. Lukowiak, A. A., Narayanan, A., Li, Z. H., Terns, R. M. & Terns, M. P. (2001) *RNA* **7,** 1833–1844.
14. Mitchell, J. R., Wood, E. & Collins, K. (1999) *Nature* **402,** 551–555.
15. Dragon, F., Pogacic, V. & Filipowicz, W. (2000) *Mol. Cell. Biol.* **20,** 3037–3048.
16. Pogacic, V., Dragon, F. & Filipowicz, W. (2000) *Mol. Cell. Biol.* **20,** 9028–9040.
17. Heiss, N. S., Knight, S. W., Vulliamy, T. J., Klauck, S. M., Wiemann, S., Mason, P. J., Poustka, A. & Dokal, I. (1998) *Nat. Genet.* **19,** 32–38.
18. Alter, B. P. & Drachtman, R. A. (1998) *Am. J. Hematol.* **58,** 298.
19. Dokal, I. (2000) *Br. J. Haematol.* **110,** 768–779.
20. Marciniak, R. A., Johnson, F. B. & Guarente, L. (2000) *Trends Genet.* **16,** 193–195.
21. Mason, P. J. (2003) *BioEssays* **25,** 126–133.
22. Vulliamy, T., Marrone, A., Goldman, F., Dearlove, A., Bessler, M., Mason, P. J. & Dokal, I. (2001) *Nature* **413,** 432–435.
23. Giordano, E., Peluso, I., Senger, S. & Furia, M. (1999) *J. Cell Biol.* **144,** 1123–1133.
24. Ruggero, D., Grisendi, S., Piazza, F., Rego, E., Mari, F., Rao, P. H., Cordon-Cardo, C. & Pandolfi, P. P. (2003) *Science* **299,** 259–262.
25. He, J., Navarrete, S., Jasinski, M., Vulliamy, T., Dokal, I., Bessler, M. & Mason, P. J. (2002) *Oncogene* **21,** 7740–7744.
26. Zhu, L., Hathcock, K. S., Hande, P., Lansdorp, P. M., Seldin, M. F. & Hodes, R. J. (1998) *Proc. Natl. Acad. Sci. USA* **95,** 8648–8653.
27. Wang, C., Query, C. C. & Meier, U. T. (2002) *Mol. Cell. Biol.* **22,** 8457–8466.
28. Moore, M. J. & Query, C. C. (2000) *Methods Enzymol.* **317,** 109–123.
29. Vulliamy, T. J., Knight, S. W., Mason, P. J. & Dokal, I. (2001) *Blood Cells Mol. Dis.* **27,** 353–357.
30. Huttenhofer, A., Kiefmann, M., Meier-Ewert, S., O'Brien, J., Lehrach, H., Bachellerie, J. P. & Brosius, J. (2001) *EMBO J.* **20,** 2943–2953.
31. Ofengand, J. & Bakin, A. (1997) *J. Mol. Biol.* **266,** 246–268.
32. Aravind, L. & Koonin, E. V. (1999) *J. Mol. Evol.* **48,** 291–302.
33. Yi, X., Tesmer, V. M., Savre-Train, I., Shay, J. W. & Wright, W. E. (1999) *Mol. Cell. Biol.* **19,** 3989–3997.
34. Tollervey, D. (1987) *EMBO J.* **6,** 4169–4175.
35. Atzorn, V., Fragapane, P. & Kiss, T. (2004) *Mol. Cell. Biol.* **24,** 1769–1778.
36. Niida, H., Matsumoto, T., Satoh, H., Shiwa, M., Tokutake, Y., Furuichi, Y. & Shinkai, Y. (1998) *Nat. Genet.* **19,** 203–206.
37. Erdmann, N., Liu, Y. & Harrington, L. (2004) *Proc. Natl. Acad. Sci. USA* **101,** 6080–6085.
38. Yaghmai, R., Kimyai-Asadi, A., Rostamiani, K., Heiss, N. S., Poustka, A., Eyaid, W., Bodurtha, J., Nousari, H. C., Hamosh, A. & Metzenberg, A. (2000) *J. Pediatr.* **136,** 390–393.
39. Knight, S. W., Heiss, N. S., Vulliamy, T. J., Aalfs, C. M., McMahon, C., Richmond, P., Jones, A., Hennekam, R. C., Poustka, A., Mason, P. J. & Dokal, I. (1999) *Br. J. Haematol.* **107,** 335–339.